# Retrieval of Cloud Properties from Ground-Based Lidar/Radiometer Data

*C.M.R. Platt, S.A. Young, R.T. Austin, S.C. Marsden,*
*G.R. Patterson, J.A. Bennett, B. Petraitis, and B. Turner*
*CSIRO, Division of Atmospheric Research*
*Aspendale, Victoria, Australia*

## Abstract

The retrieval of cloud properties from Lidar/Radiometer data by the LIRAD method is described. Several data sets taken by the CSIRO Division of Atmospheric Research are now available for such retrievals as a result of several major field experiments during the past six years.

The LIRAD method is reviewed briefly and its application to the various data sets is described. The data have been obtained at temperatures ranging from +5°C down to -80°C, representing a large fraction of global atmospheric temperatures. Results include information on cloud height and depth, infrared emittance and linear depolarization ratio, together with functions that relate the lidar to the IR data and that lead to information on both particle size and habit.

The methods developed have been demonstrated to be suitable for processing large amounts of cloud data in what could be close to real time. Thus, the methods should be suitable for retrieving detailed cloud optical and microphysical properties from cloud lidar and infrared data now being obtained at the ARM Southern Great Plains (SGP) Cloud and Radiation Testbed (CART) site.

The design and construction of a new ARM/CSIRO Mark II radiometer that employs a Stirling Cycle cooler has now been completed. It is described briefly.

## Introduction

The Lidar/Radiometer (LIRAD) method was originally developed at the CSIRO Division of Atmospheric Research in order to retrieve detailed properties of cirrus clouds from ground-based observations. The LIRAD method has been described fully in Platt et al. (1987) and earlier papers. It has also been described in recent ARM Science Team proceedings and in Platt et al. (submitted).

In short, a lidar is used to measure cloud height, depth (when the cloud is semitransparent), phase, and structure; and a narrow-beam spectral radiometer measures the cloud infrared radiance in a selected spectral band about 1 µm wide in the atmospheric window (8 to 13 µm), where infrared absorption and emission from the water vapour in the atmosphere are minimal. Both instruments normally point in the vertical. It is also necessary to obtain radiosonde profiles of temperature and humidity at regular intervals.

The products obtained are the cloud infrared emittance and optical depth, the optical depth at the lidar wavelength, and the profiles of infrared absorption coefficient and lidar extinction coefficient. Information on cloud particle habit and cloud effective particle size is also obtained.

To obtain the cloud infrared emittance in the detected spectral band, it is necessary to assume a value for the ratio between the cloud lidar backscatter coefficient and the infrared absorption coefficient. This value is at present assumed to be constant within one particular cloud profile. Radiosonde-derived values of atmospheric temperature are ised tp calculate blackbody radiances and infrared optical depths at a number of height intervals in the cloud. The cloud radiance at cloud base is then calculated from an equation of radiative transfer. This radiance is then compared with the surface-measured radiance to obtain a cloud emittance and optical depth. However, the surface radiance must first be corrected for water vapour absorption and emission between the cloud and the ground. This is achieved by employing an equation of radiative transfer, together with values of temperature and humidity derived from the radiosonde data.

Values calculated by Platt and Stephens (1980) are used to make corrections for scattering of radiation inside the cloud, as well as for radiation that is emitted upwards at the earth's surface and reflected down again by the cloud. Although the infrared reflectivity, or albedo, of the cloud may typically be only a few percent, the difference between the ground and the cloud temperatures—and therefore their blackbody radiances—ensures that the reflected radiance is a significant component of the total. For tropical clouds, the reflected radiation can be as much as 20% of the total cloud radiance (Platt et al.1984). The scattering corrections are checked by ensuring that the cloud emittance approaches unity as the cloud optical depth increases.

Further information on the cloud microphysics can be obtained by plotting the lidar height-integrated attenuated cloud backscatter $\gamma'$ against the cloud infrared emittance $\epsilon$. These two quantities can be related by an equation of the type (Platt 1979):

$$\gamma' = \frac{k}{2\eta}\left(1 - \exp\left(-2\alpha\eta \log\frac{1}{1-\varepsilon}\right)\right) \tag{1}$$

where $\eta$ is a multiple scattering factor and $\alpha$ is the ratio between the optical depth at the lidar wavelength and the infrared absorption optical depth at the radiometer wavelength. Now, the cloud backscatter to extinction ratio, k, is numerically equal to the backscatter phase function. Because this latter quantity is sensitive to the crystal type, a measure of k gives information on ice crystal habit (Macke 1992). The quantity k can be inferred from Equation 1 when the emittance $\epsilon$ tends to 1. This requires an estimate of the quantity $\eta$. Some calculations made by Platt (1981) indicate that $\eta$ decreases with the cloud altitude. The expression

$$\eta = 0.72 + 6 \times 10^{-3}T \tag{2}$$

describes the variation of $\eta$, where T is the cloud temperature (°C). $\eta$ varies from 0.72 at 0°C to 0.24 at -80°C. The uncertainty in the formula of Equation 2 is about 30%, due to the neglect of the effects of other variables such as optical depth (Platt 1981).

The quantity $k/2\eta$ is also employed to correct the lidar cloud backscatter for attenuation in the cloud. The cloud optical depth $\delta$ can then be obtained from the equation

$$\delta = \frac{\gamma}{k}. \tag{3}$$

where $\gamma$ is the corrected cloud integrated backscatter.

It is necessary to use values of $\eta$ from Equation 2 in order to obtain a value of k. Optical depths less than 2 or 3 in value can be obtained with reasonable accuracy.

Finally, the quantity $\alpha$ gives information on the particle size. Calculating Equation 1 for various values of $\alpha\eta$ yields the curves given in Figure 1, where $\alpha\eta$ varies from 1.5 to 0.75. Theoretical calculations by Platt (1979) indicate that a variation in $\alpha$ of from 3.0 to 1.5 corresponds to a variation in crystal diameter of from 5 µm to 100 µm. Variations in $\eta$ must also be considered, however, and these aspects are being studied at present.

For tropical sites, the water vapour absorption and emission become very significant, water vapour emission often being greater than cloud emission, and special methods using microwave observations of water vapour path have been employed to correct for water vapour effects. The depolarisation ratio in the backscattered lidar returns has also been measured, and this leads to further information on cloud particle type.

## Data Sets

Three data sets have been used to investigate cloud optical and microphysical properties over a range of temperature from +5°C to -80°C:

a. *Experimental Cloud Lidar Pilot Study (ECLIPS).* Aspendale, Victoria.

b. *The ARM Pilot Radiation Observation Experiment (PROBE)*, Kavieng, Papua New Guinea.

c. *Midlatitude Summer and Winter data and tropical data (LIRAD)*, Aspendale, Victoria and Darwin, Northern Territory.

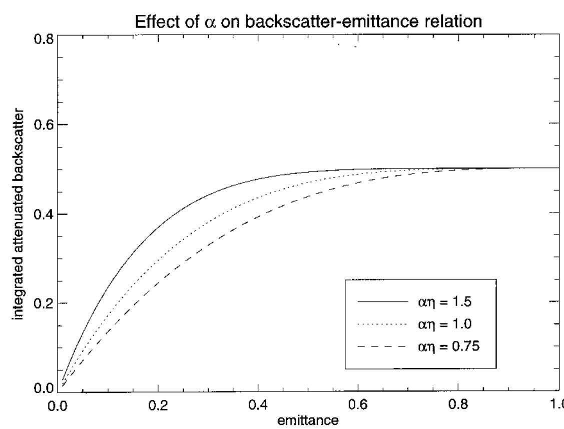


**Figure 1**. A plot of integrated attenuated backscatter $\gamma'$ versus infrared emittance $\epsilon$ (10.86 µm) for different values of the ratio $\alpha$.

These data have all been processed to obtain the various quantities mentioned above. The original LIRAD results were published in Platt et al. (1987), and other data have been submitted for publication (Platt et al., submitted). Here we select a few examples to illustrate the method.

# Results

A plot of $\gamma^{/}$ versus $\epsilon$ from ECLIPS data for a high temperature range is shown in Figure 2 and from PROBE, for a lower range, in Figure 3. Features are the lower values of $k/2\eta$ for the colder clouds, but the higher value of $\alpha$ compared to the cloud of Figure 2.

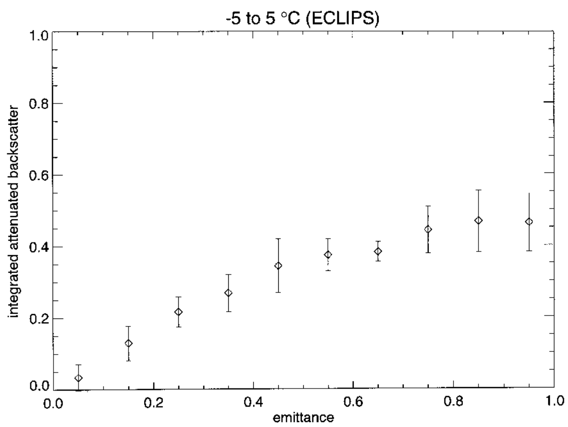


**Figure 2**. A plot of integrated attenuated backscatter $\gamma^{/}$ versus infrared emittance $\epsilon$ (10.86 µm) for clouds in the temperature range -5°C to +5°C from the ECLIPS project.

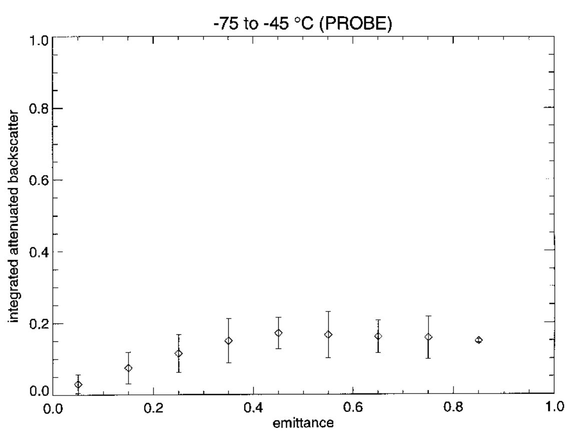


**Figure 3**. A plot of integrated attenuated backscatter $\gamma^{/}$ versus infrared emittance $\epsilon$ (10.86 µm) for clouds in the temperature range -75°C to -45°C from the PROBE project.

The intercepts from Figures 2 and 3 when $\epsilon$ tends to unity are 0.47and 0.16, respectively. Applying Equation 2 yields a k value of 0.68 at about 0°C and 0.08 at -75° to -45°C. The former value is close to what Deirmendjian (1969) predicts for a water cloud, whereas the latter is a value typical of a solid bullet (Macke 1992). Thus, the cloud microphysics can be broadly delineated.

Also, according to Figure 1, the colder cloud has a higher value of $\alpha\eta$, although it is not obvious how this relates to particle size because changes in the value of $\eta$ with temperature will tend to lessen the effects of a change in $\alpha$ (see Platt et al. submitted).

Some of the results from PROBE reported in the ARM proceedings of the 1995 Science Team meeting have subsequently been found to be in error. This error was due to a faulty calibration that has since been corrected. In short, the curves of$\gamma^{/}$ versus $\epsilon$ for temperatures greater than about -40°C showed a local maximum in $\gamma^{/}$ around about an emittance of 0.4. A correction to the analyzed data has removed this maximum to give the normal steady increase in temperature. The results will be reported in detail in Platt et al. (submitted).

Figure 4 shows how the infrared emittance at 10.86 µm increases with temperature. This covers a greater range of temperatures than previously was available. The scatter is quite large, indicating that the cloud emittance cannot be obtained precisely from a measurement of cloud temperature. Clouds are very inhomogeneous, and at any single temperature, there will be a distribution of emittances about some mean. However, the observed temperature tendencies are still useful for validating numerical models, which are themselves still very imprecise.

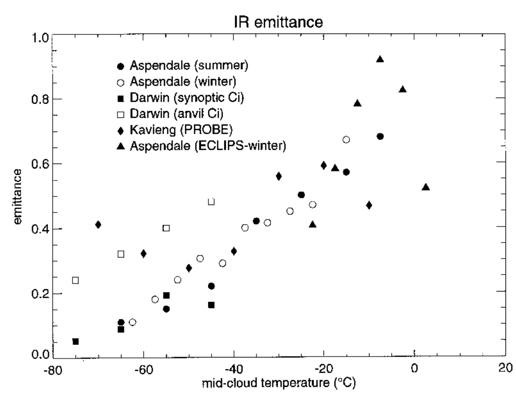


**Figure 4**. Plot of emittance $\epsilon$ (10.86 µm) against mid-cloud temperature for clouds observed in various experiments.

## A New Radiometer with a Stirling Cycle-Cooled Detector

A second, Mark II, spectral narrow-beam radiometer has been designed and fabricated at the CSIRO Division of Atmospheric Research. The aim of this second design was to allow the radiometer to run continuously with minimum attention. The Stirling Cycle-cooled detector allows operation at liquid nitrogen temperatures without the need to fill the detector dewar repeatedly.

The optical system is essentially the same as for the previous Mark I, which was found to be quite satisfactory. The final stage of the optics has been improved, however, to allow the optical beam to be precisely positioned and focused onto the millimeter-square detector. The system also has a built-in 486 computer and hard disk and a dual voltage power supply.

The ARM Mark II radiometer with and without its cover is shown in Figures 5 and 6. Tests on the radiometer are being carried out at present, including comparisons with the Mark I radiometer. According to the manufacturer's specifications, the Mark II should operate for up to a year before maintenance of the Stirling Cycle cooler is required.

## Summary

Detailed optical and structural properties of clouds, particularly high clouds, can be retrieved using the LIRAD method. The method will now be improved and modified to allow retrieval of cloud optical properties in near real time from an ARM CART site. Results obtained thus far can be used as a benchmark to compare with cloud optical properties obtained on a more continuous basis in the future.

**Figure 5**. The new CSIRO/ARM Stirling Cycle cooler with its cover on.

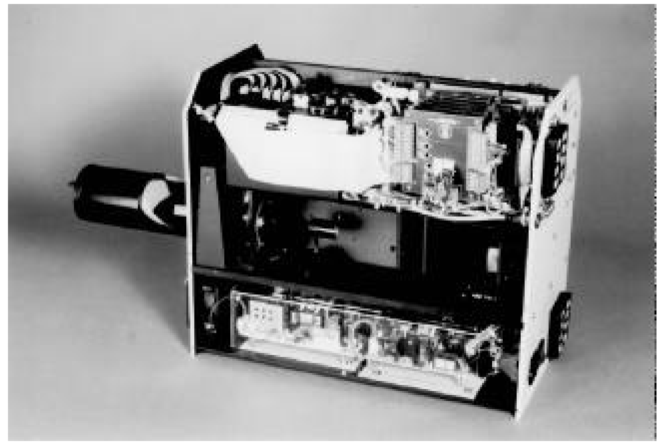

**Figure 6**. Same as Figure 5, but with the cover off.

A new narrow-beam fast filter radiometer has now been developed using a Stirling Cycle cooler for the detector. After further modifications, the radiometer will be ready for use at a CART site.

## References


Deirmendjian, D., 1969: *Electromagnetic scattering on spherical polydispersions*. Elsevier, NY, London, Amsterdam.

Macke, A., 1992: "Scattering of light by polyhedral ice crystals." *Appl. Opt.*, **32**:2780-2788.

Platt, C.M.R., 1979: "Remote sounding of high clouds. Part I: Calculation of visible and infrared optical properties from lidar and radiometer measurements." *J. Atmos. Sci.*, **18**:1130-1143.

Platt, C.M.R., and G.L. Stephens, 1980: Radiative properties of cirrus clouds in the infrared region. *J. Atmos. Sci.*, **37**:435-446.

Platt, C.M.R., 1981: "Remote sounding of high clouds. Part III: Monte Carlo calculations of multiply scattered lidar returns." *J. Atmos. Sci.*, **38**:156-167.

Platt, C.M.R., A.C. Dilley, J.C. Scott, I.J. Barton, and G.L. Stephens, 1984: "Remote sounding of high clouds. Part V: Infrared properties and structures of tropical thunderstorm anvils." *J. Clim. Appl. Meteorol.*, **23**:1296-1308.

Platt, C.M.R., J.C. Scott, and A.C. Dilley, 1987: "Remote sounding of high clouds. Part VI: Optical properties of mid-latitude and tropical cirrus." *J. Atmos. Sci.*, **44**:729-747.

Platt, C.M.R., S.A. Young, P.J. Manson, G.R. Patterson, S.C. Marsden, and J. Churnside: "The optical properties of equatorial cirrus from observations in the ARM Pilot Radiation Observation Experiment." Submitted to *J. Atmos. Sci.*